Cogn Neurodyn (2011) 5:333–342
DOI 10.1007/s11571-011-9158-9

RESEARCH ARTICLE

Spatiotemporal characteristics of synaptic EPSP summation on the dendritic trees of hippocampal CA1 pyramidal neurons as revealed by laser uncaging stimulation

Makoto Yoneyama · Yasuhiro Fukushima · Minoru Tsukada · Takeshi Aihara

Received: 16 February 2011 / Revised: 31 May 2011 / Accepted: 7 June 2011 / Published online: 18 June 2011

Abstract Synaptic strength is modified by the temporal coincidence of synaptic inputs without back-propagating action potentials (BPAPs) in CA1 pyramidal neurons. In order to clarify the interactive mechanisms of associative long-term potentiation (LTP) without BPAPs, local paired stimuli were applied to the dendrites using high-speed laser uncaging stimulation equipment. When the spatial distance between the paired stimuli was <10 micrometer, nonlinear amplification in excitatory postsynaptic potential summation was observed. In the time window from −20 to 20 ms, supralinear amplification was observed. Supralinear amplification was modulated by antagonist of voltage-gated Na^+/Ca^{2+} channels and NMDA-type glutamate receptors. These results are closely related to the spatio-temporal-characteristics of associative LTP without BPAPs. This study proposes an essential aspect of dendritic information processing.

Keywords Hippocampus · Dendrite · EPSP summation · Uncaging · Supralinear amplification · Spatiotemporal information

M. Yoneyama · Y. Fukushima · M. Tsukada · T. Aihara (✉)
Brain Science Institute, Tamagawa University, 6-1-1 Tamagawagakuen, Machida, Tokyo 194-8610, Japan
e-mail: aihara@eng.tamagawa.ac.jp

T. Aihara
Faculty of Engineering, Tamagawa University, Machida, Tokyo, Japan

Y. Fukushima
Faculty of Health and Welfare, Kawasaki University of Medical Welfare, Kurashiki, Okayama, Japan

Introduction

Hebb (1949) proposed the idea that synaptic strength is enhanced when pre- and post-synaptic neurons are activated simultaneously (Hebb's rule). One piece of experimental evidence for Hebb's rule is spike timing-dependent plasticity (STDP), in which the order and relative timing of pre- and post-synaptic spiking determines the direction of plasticity (Bi and Poo 1998; Nishiyama et al. 2000; Tsukada et al. 2005; Dan and Poo 2006). Positive timing is when the excitatory postsynaptic potential (EPSP) precedes the postsynaptic action potential (AP) while negative timing is when the EPSP follows the AP. For hippocampal neurons in dissociated culture, positive timing induces long-term potentiation (LTP), whereas negative timing induces long-term depression (LTD). These results show the temporal asymmetry of plasticity caused by a difference in the input–output order of activation (Bi and Poo 1998). Tsukada et al. (2005) reported symmetric plasticity of STDP in a hippocampal CA1 slice preparation, caused by an inhibitory network controlled by GABAergic interneurons.

LTP induction by input–input association without back propagating action potentials (BPAPs) has been observed as a non-Hebb learning rule in hippocampal CA1 pyramidal neurons (Tsukada et al. 2007). This type of LTP was named "heterosynaptic associative LTP". Huang et al. (2004) reported that temporal coincident input of paired stimuli (strong and weak input) induces LTP in both strong and weak pathways (heterosynaptic associative LTP). Heterosynaptic associative LTP was also observed when BPAPs were blocked by low-level TTX application (Tsukada et al. 2007). These results show that a BPAP is not necessary for heterosynaptic associative LTP induction. This data is an important motivator for Tsukada's

spatiotemporal learning rule (STLR) (Tsukada et al. 1996, 2007). In heterosynaptic associative LTP, the temporal coincidence of a strong input (which can induce LTP alone) and a weak input (which cannot induce LTP alone) can induce LTP in the weak input pathway (Huang et al. 2004; Tsukada et al. 2007). Heterosynaptic associative LTP has the characteristic feature of an interaction of strong and weak inputs. However, few studies of the association of the interactions of two inputs at the intracellular recording level have been done.

Recently, two papers concerning the basic mechanism of associative LTP have been published. Cash and Yuste (1999) reported that the associative property of EPSP summation, when the distance between two input sites (Δd) was more than 50 μm, was linear or sub-linear on dendrites. Gasparini and Magee (2006) reported supralinear amplification of EPSP summation on dendrites when 7 inputs with similar peak amplitudes were applied to dendrites within an area of 25 μm during a 3-ms interval. However, Cash and Yuste (1999) did not show the association property near the soma (<50 μm) or for $\Delta d < 50$ μm, and Gasparini and Magee (2006) did not examine the detailed spatiotemporal properties of the supralinear association.

In this study, the interaction mechanism of EPSP for two independent inputs was investigated in order to clarify basic mechanism for associative LTP without BPAPs. Local stimulation was applied to the dendrite using high-speed uncaging equipment and the sub-threshold postsynaptic membrane potential without AP induction was recorded by the whole cell patch-clamp method. Detailed spatiotemporal properties were examined: the distance between the two inputs was varied from 5 to 40 μm and the input timing difference was varied from −20 to 40 ms.

Materials and methods

All experiments were approved by the Tamagawa University Animal Care and Use Committee.

Animals and brain slices

Hippocampal slices were prepared from Wister rats (P14-21) as described previously (Tsukada et al. 2005). Rats were anesthetized, the brain was quickly removed from the skull, and placed into cold artificial cerebrospinal fluid (ACSF) containing 142 mM NaCl, 2 mM $MgSO_4$, 5 mM KCl, 2.6 mM NaH_2PO_4, 2 mM $CaCl_2$, 26 mM $NaHCO_3$, and 10 mM glucose bubbled with 95% O_2 and 5% CO_2. The brain was sliced at an angle of 30°–45° along the long axis of the hippocampus, with a thickness of 300 μm. Slices were kept in ACSF at room temperature for at least 60 min before recording. During recording, in order to block the $GABA_A$ receptor mediated current, 25 μM of picrotoxin (Sigma) was added to the ACSF.

Stimulation with high-speed uncaging equipment

Stimulation was applied using a laser confocal microscope with high-speed UV-laser uncaging equipment (Kojima et al. 2006) custom-built by Carl-Zeiss (Germany). The radius of the laser irradiation spot was <1 μm. To visualize the arborization of dendrites, Oregon Green BAPTA-1 (OGB-1, Molecular Probes) was added to the pipette solution and absorbed into the cell for 10 min. Dendrites were visualized using an argon laser (488 nm) with a confocal laser scan microscope. MNI-caged glutamate (final concentration: 125 μM, Tocris) was added to the ACSF before the laser uncaging stimulation. The UV laser irradiated the dendrite in the stratum radiatum near the soma (Fig. 1a). The duration of laser irradiation was 1 ms, and laser power was adjusted so that the peak amplitude of unitary EPSP was 1–1.3 mV. With this unitary EPSP amplitude, none of the stimulus patterns induced APs. In the hippocampal CA1 area, stimulation to a single synapse induces an EPSP with a 0.2 mV peak, which was not dependent on dendritic site (Magee and Cook 2000). Therefore, the unitary EPSP (1–1.3 mV) in this study is believed to involve responses from 5 to 7 synapses.

Experiment 1

In order to clarify the spatial properties of EPSP summation on dendrites, paired stimuli were applied to 2 sites (5, 10, 15, 20, 40, 45, 50, 55, and 60 μm away from soma) on a dendrite. Two types of stimulation pattern were defined (Fig. 1c), corresponding to the types of stimulation used in studies of heterosynaptic associative LTP (Huang et al. 2004; Tsukada et al. 2007). Strong and weak stimulations involve 3 pulses (at 10-ms intervals) and 1 pulse, which induce three and one unitary EPSPs, respectively (Fig. 1c(1)).

Three types of electrical stimulation sets were used in this study (Fig. 1b). Two stimulation sets consist of a strong and a weak input: in Type 1 the strong input is applied to the proximal site and the weak input to the distal site (Fig. 1b left); in Type 2 the strong input is applied to the distal site and the weak input to the proximal site (Fig. 1b middle). The other type (Type 3) consists of weak inputs applied to both sites (Fig. 1b right). Individual strong or weak stimulation was applied for linear summation, as a control (Fig. 1c(2)). To reduce the sequential effects of stimulation, the order of the stimulation sequence was chosen randomly for each neuron.

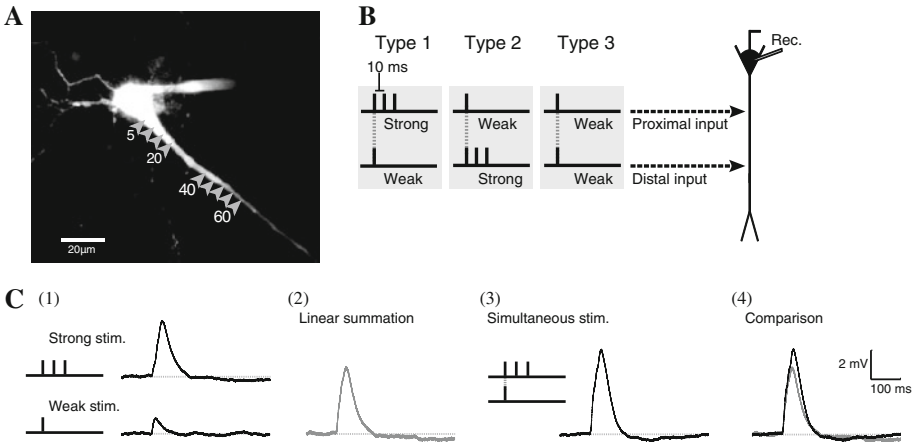

Fig. 1 Experimental protocols. **a** Image of hippocampal CA1 neuron visualized with Ca^{2+} sensitive dye (OGB-1). *Arrow heads* indicate stimulations sites and the numbers below the *arrow heads* indicate the distance from the soma (μm). **b** Three types of electrical stimulation set. Two stimulation sets consist of a pair of strong (three pulses at 10-ms intervals) and weak (one pulse) stimulation: in Type 1 there is strong input to the proximal site and weak input to the distal site; in Type 2 there is strong input to the distal site and weak input to the proximal site; Type 3 consists of weak inputs to both sites. **c** Comparison between the traces from paired stimuli and sum of the traces of the two individual stimulations. Each trace indicates (*1*) responses by strong and weak stimulation individually, (*2*) sum of the two traces shown in (*1*), (*3*) Response by paired stimuli, and (*4*) overlay of traces shown in (*2*) and (*3*)

Experiment 2

To clarify the spatial area dependency of stimulation sites, paired stimuli were applied to the proximal area (5–30 μm from the soma, Fig. 4a top) or the distal area (30–60 μm from the soma, Fig. 4a bottom). Stimuli pairs of Type 1, 2, and 3 were used, and the distance between two stimulation sites (Δd) was 5, 10, or 15 μm.

Experiment 3

To clarify the molecular mechanism of supralinear amplification, a pharmacological experiment was conducted. An antagonist was added to the ACSF: AP-5 (100 μM, Sigma) for the NMDA-type glutamate receptor; TTX (0.5 μM, Wako Chemicals, Japan) for the voltage-gated Na^+ channel; or $NiCl_2$ (50 μM, Kanto Chemicals, Japan) for voltage-gated Ca^{2+} channel. Paired stimuli in Type 3 were applied to the proximal area (5–30 μm from the soma) at $\Delta d = 5$ or 10 μm.

Experiment 4

To clarify the temporal dependence on input timing, paired stimuli were applied at temporally inconsistent timings (5 and 15 μm from the soma, $\Delta d = 10$ μm, Fig. 5a). The onset of strong stimulation was fixed, and the timing of weak stimulation was shifted by −20, −10, 0, +10, +20, +30, and +40 ms (Fig. 6b). Types 1 and 2 paired stimuli were used.

Recording

Patch-clamp recordings were made from CA1 pyramidal neurons. The recording electrode was a micro glass pipette made using a puller. The resistance of the electrode was 5–8 MΩ. The patch solution contained 120 mM $KMeSO_4$, 20 mM KCl, 10 mM HEPES, 10 mM EGTA, 4 mM Mg_2ATP, 0.3 mM TrisGTP, 14 mM $Tris_2$phosphocreatine, and 4 mM NaCl (pH 7.25 with KOH). To visualize the dendrites, OGB-1 was added to the patch solutions (final concentration was 100 μM). Neural responses were recorded using the whole-cell patch clamp method (current-clamp mode). A patch clamp amplifier (EPC-7plus, Heka) was used for recording. Neurons whose starting membrane potential was <−50 mV were used for experiment. The membrane potential was adjusted to be -70 ± 1.5 mV by current injection. The neural response was high-cut filtered at 5 kHz and stored at 48 kHz using personal computer software (Clampex 9.2, Molecular Devices).

Analysis

In one neuron, three responses to the paired stimuli were averaged and used as representative data. The resting membrane potential from 800 to 300 ms before the stimulation was averaged and defined as 0 mV. The waveforms of EPSPs induced by individual strong or weak inputs (Fig. 1c(1)) were summed (Fig. 1c(2)) by adjusting the onset timing of stimulation. As shown in Fig. 1c(4), the linear EPSP sum (Fig. 1c(2)) was compared to the EPSP

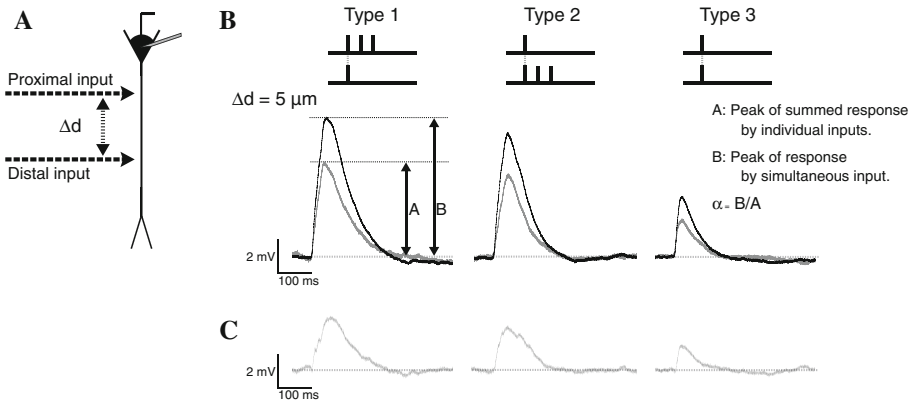

Fig. 2 Nonlinear amplification by three stimulation sets. **a** Schematic diagram of stimulation sites. The distance between two stimulation sites is defined as Δd. **b** Examples of responses to the three stimulation sets at $\Delta d = 5$ μm. *Black* and *gray lines* indicate responses to paired stimuli and the sum of the responses to the two individual inputs, respectively. The peak of amplitude of the response to paired stimuli and sum of two responses are defined as (*A*) and (*B*) in the figure, respectively. The amplification rate (α) was defined as $\alpha = B/A$. **c** The difference between the response to paired stimuli and the sum of individual responses

induced by paired stimuli (Fig. 1c(3)). The decay time constant (τ) was the time for the membrane potential to fall from its peak to 1/e of the peak potential in the subtracted trace (Fig. 2c). The statistical analysis used ANOVA and $P < 0.05$ was used as the significance level.

Results

Responses by paired stimuli and sums of individual stimulation

Figure 2 shows examples of EPSPs from 3 types of paired stimuli and the sums of EPSPs from individual inputs. The distance between the two stimulation sites on the dendrite (Δd) was 5 μm (Fig. 2a). Effect of supralinear amplification by paired stimuli was measured as an "amplification ratio" (α), which was defined as the ratio of the peak amplitude of the response to paired stimuli divided by the peak amplitude of the linear sum of responses to individual stimulation (Fig. 2b). In Fig. 2c the subtracted traces show the supralinear amplification produced by paired stimuli.

Spatial pattern dependency

Figure 3 shows the distance dependency of supralinear amplification by paired stimuli (Experiment 1, n = 36). For any type of paired stimuli, significant amplification was observed ($\alpha > 1$) at $\Delta d = 5$, and 10 μm. At $\Delta d = 15$, and 20 μm, significant amplification was not observed ($\alpha \approx 1$). At $\Delta d = 40$ μm, significant amplification was not observed for Type 2 and 3 pairs of stimuli, but a sub-linear summation effect ($\alpha < 1$) was observed for Type 1 pairs. At $\Delta d = 40$ μm, the summation effect was only linear ($\alpha \approx 1$) or significantly decreased ($\alpha < 1$), which agrees

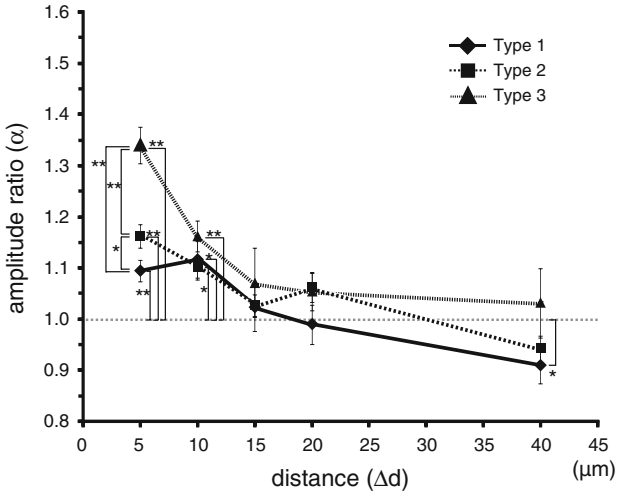

Fig. 3 Distance dependency of amplification by paired stimuli. The Y-axis indicates the amplification (α), the X-axis indicates the distance between the two stimulation sites (Δd). The symbols in the graph indicate the type of stimulation: Type 1 (*filled diamond*); Type 2 (*filled square*); and Type 3 (*filled triangle*). *Error bars* indicate the standard error of the mean and *asterisks* indicate the level of significance: * $P < 0.05$ and ** $P < 0.01$

with the results of a previous study (Cash and Yuste 1999). Our results show that supralinear amplification is observed when Δd is <10 μm, but is not observed when Δd is more than 15 μm.

The dependency of supralinear amplification on paired stimuli type (Types 1, 2, and 3) was examined. At $\Delta d = 5$ μm significant differences of amplification ratio were observed (mean ± SE): Type 3 (139 ± 4%) > Type 2 (118 ± 2%) > Type 1 (111 ± 2%). These results show that the amplification ratio was dependent on the stimulus pattern (combination of proximal or distal, and strong or weak input) when Δd is short. Considering the fact that

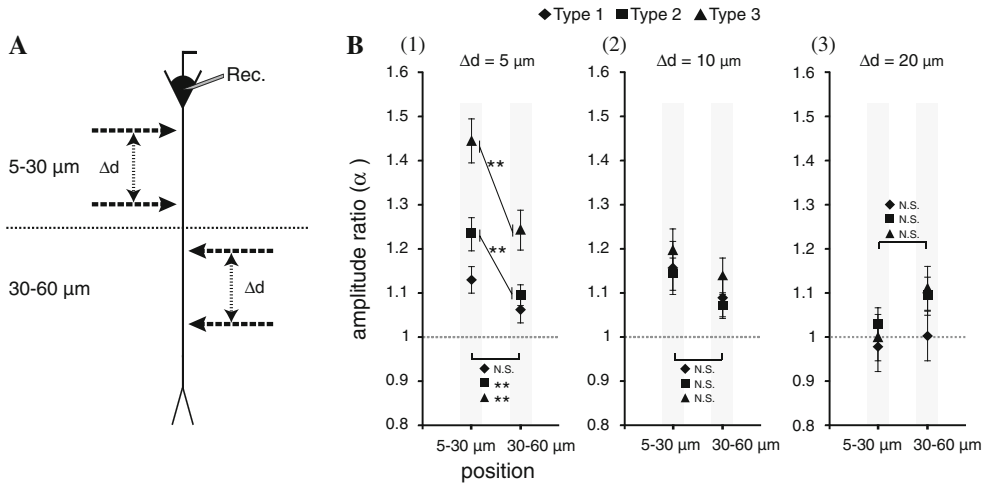

Fig. 4 Dependency of amplification of the area of stimulation sites. **a** The dendritic area 5–30 μm away from the soma was defined as the proximal area, and the area 30–60 μm away was defined as the distal area. Paired stimuli were applied in both areas. **b** The graphs of area dependency for (*1*) $\Delta d = 5$ μm, (*2*) $\Delta d = 10$ μm, and (*3*) $\Delta d = 20$ μm. The *Y*-axis indicates the amplification ratio (α), and the *X*-axis indicates the stimulation area. The *symbols* in the *graph* indicate the type of stimulation: Type 1 (*filled diamond*), Type 2 (*filled square*), and Type 3 (*filled triangle*). The *errors bar* indicate standard errors of the mean and *asterisks* indicate the level of significance: ** $P < 0.01$

Type 3 (weak–weak) paired stimuli show the strongest supralinear amplification, it appears that the interaction between the weak input and the first of the three pulses in the strong input at coincident timing was the strongest due to temporal coincidence. In contrast, the interaction between the weak input and the second or third pulses in the strong input at inconsistent timings was relatively small.

Next, in order to clarify area dependency of stimulation sites, paired stimuli ($\Delta d = 5$, 10, 20 μm) were applied to the proximal (5–30 μm from the soma) or distal (30–60 μm from the soma) areas on the dendrite (Experiment 2, $n = 15$ in proximal area, $n = 12$ in distal area, see Fig. 4a). Figure 4b shows that, at $\Delta d = 5$ μm, the amplification ratios for Type 2 and 3 pairs in the proximal area were significantly larger than those in the distal area and that the supralinear amplification effect in the proximal area was larger than that in the distal area when Δd was short but the effects were similar when Δd was sufficiently large.

Molecular mechanisms for supralinear amplification

Pharmacological effects on the amplification ratio were examined by adding channel blockers to the ACSF (Experiment 3, Fig. 5). A normalized amplification ratio ($\Delta\alpha$) was defined relative to the amplification ratio with normal ACSF which was defined as 100%. At $\Delta d = 5$ and 10 μm, $\Delta\alpha$ was significantly reduced when Ni^{2+} or TTX was added to the ACSF (Fig. 5b, c). When AP-5 was added to the ACSF, no significant difference was observed.

Furthermore, the decay time constant (τ) was measured from the subtracted trace (Fig. 2c) corresponding to a specific increment in supralinear amplification. The decay time constant was measured at $\Delta d = 5$ and 10 μm, when significant supralinear amplification was observed. The decay time constant in normal ACSF was defined as 100% (leading to a normalized time constant ratio, $\Delta\tau$). To clarify the effect of channel blockers, time constant ratios at $\Delta d = 5$ and 10 μm were measured. The value of $\Delta\tau$ was significantly reduced when AP-5 was added to the ACSF (Fig. 5d), but no significant difference was observed for any other condition. The decay time constant at $\Delta d = 5$ μm was $\tau = 69.7 \pm 2.9$ ms (mean ± SE) in normal ACSF, $\tau = 66.2 \pm 9.1$ ms with TTX ($n = 6$), $\tau = 60.5 \pm 4.0$ ms with Ni^{2+} ($n = 5$), and $\tau = 46.6 \pm 5.8$ ms in ACSF with AP-5 ($P < 0.05$) ($n = 7$). There were no significant differences at $\Delta d = 10$ μm.

Temporal dependency of input timing

The dependence of EPSP interaction on the temporal relation of paired stimuli was examined (Experiment 4). The onset of the strong input was fixed, and onset timing of the weak input was shifted (Δt) relative to that by −20 to +40 ms in 10 ms steps (see Fig. 6a,b). Figure 6c shows an example of the results for Type 1 pairs. Supralinear amplification was observed at $\Delta t = -20, -10, 0, +10$, and +20 ms. Figure 6d shows a summary of the results for Type 1 and Type 2 pairs ($n = 7$). Supralinear amplification was observed for timings from $\Delta t = -20$ to +20 ms for

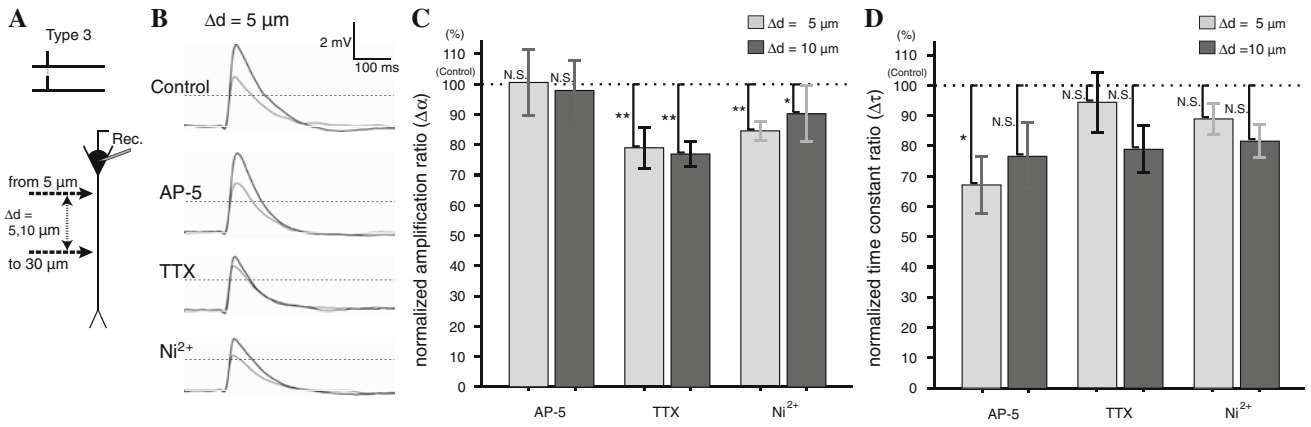

Fig. 5 Effects of channel blockers, AP-5, TTX, and Ni^{2+}. **a** A schematic drawing of the experiment. Type 3 paired stimuli were applied to the proximal area at $\Delta d = 5$ or 10 μm. **b** The effects of channel blocker application at $\Delta d = 5$ μm. *Black* and *gray lines* indicate the traces for paired stimuli (Type 3) and the linear summation of individual inputs. **c** The *graphs* summarize the effects of channel blocker application at $\Delta d = 5$ and 10 μm. The *Y*-axis indicates the supralinear amplification ratio (Δα, see text). **d** The time constant ratio (Δτ, see text) at $\Delta d = 5$ and 10 μm. *Error bars* indicate the standard error of the mean and *asterisks* indicate the level of significance: * $P < 0.05$ and ** $P < 0.01$

Type 1 pairs (Fig. 6d, left), and for timings from $\Delta t = -10$ to +20 ms for Type 2 pairs (Fig. 6d, right). These results suggest supralinear amplification have a well-defined time window from −10 to +20 ms (30 ms width).

In addition, a type dependency was observed at $\Delta t = -20$ ms: supralinear amplification was observed in Type 1 but not in Type 2 (Fig. 6d). This suggests that the timing dependency of supralinear association was affected by the sites of the strong and weak input pair. When the onset of the weak input was earlier than that of the strong input ($\Delta t = -20$ and −10 ms), supralinear amplification was observed. On the other hand, when the onset of the strong input was earlier than that of the weak input ($\Delta t = +30$ and +40 ms), supralinear amplification was not observed. This suggests that the timing dependence of the supralinear amplification shows an asymmetry with respect to the order of the weak and strong inputs in paired stimuli.

Figure 6e shows the statistical differences between the responses to paired inputs with various timings and the sum of the responses to individual strong and weak inputs at $\Delta t = 0$ ms. In Type 1 and Type 2 pairs, significant amplification by paired stimuli was observed for $\Delta t = 0$, +10, and +20 ms (Fig. 6e). In Type 2 pairs, a significant reduction was observed at $\Delta t = -20$ and +40 ms. The timing dependency for Type 2 pairs, therefore, has a sharper, "Mexican hat"-like, time window than for Type 1 pairs.

Next, the latency to the peak amplitude of the EPSP, whose starting time was adjusted to match the onset of the strong input, was measured for paired stimuli (Fig. 6f). No statistically significant effect was observed for any type of paired stimuli from $\Delta t = -20$ to +20 ms, but a significant delay was observed for $\Delta t = +30$ and +40 ms.

Discussion

Spatial properties of EPSP summation on a dendrite

Cash and Yuste (1999) revealed that the EPSP summation rule was linear or sub-linear depending on the input sites of the dendrite by using a puff of glutamate. However, the application area of glutamate was not restricted because they used the puff technique. In addition, they did not examine the detailed spatial properties of EPSP summation, when the distance between two stimulation sites was 50 μm or less. In Gasparini and Magee (2006), 7 input pulses at 3-ms intervals within a 25 μm length on a dendrite induced supralinear amplification of EPSP summation by a local spike. However, they did not examine the detailed spatial dependence on the distance between the two input sites (Δd). In addition, they did not examine the summation property of the dendrite near the soma (<50 μm). In this paper, we have clarified the detailed spatial properties of EPSP summation near the soma using high-speed laser uncaging equipment (Experiment 1, Fig. 3). Our results indicate that EPSP summation by paired stimuli was significantly larger than a linear sum of EPSPs from individual weak and strong inputs. This is the supralinear amplification effect of EPSP summation on a dendrite. Supralinear amplification was dependent on Δd, and was observed when Δd is 10 μm or less. When Δd was 15 μm or more, the EPSP sum was linear. This result is consistent with the result of Cash and Yuste (1999), which shows a linear summation on dendrites when Δd is more than 50 μm. Our results give a quantitative-assessment of the distance dependence of EPSP summation, which was not shown by Gasparini and Magee (2006).

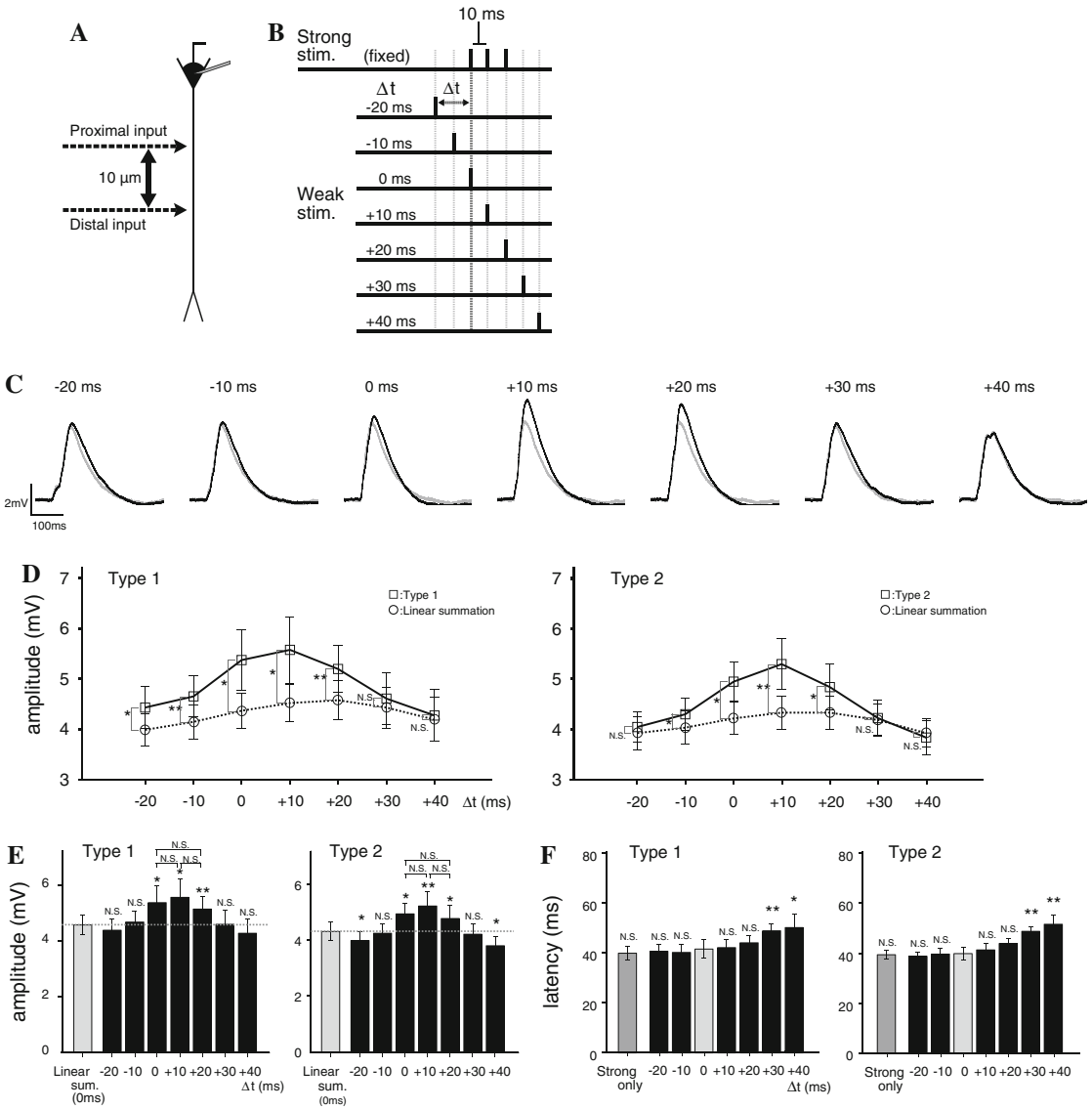

Fig. 6 Dependence on input timing. **a** Schematic diagram of stimulation sites. The distance (Δd) was fixed at 10 μm. **b** Schematic drawing of the timing of the two inputs. The timing of the strong input was fixed, and the timing of the weak input was shifted relative to that by −20 to +40 ms in 10 ms steps. **c** Examples of responses to Type 1 stimulation at each input timing. *Black* and *gray lines* indicate the response to paired stimuli and the sum of responses to the two individual inputs, respectively. **d** The graph of input timing dependency of amplification rate for Type 1 (*left*) and Type 2 (*right*) stimulation sets. The *Y*-axis indicates peak amplitude (mV), and the *X*-axis indicates the timing of the weak input (Δt). The responses to paired stimuli are shown as *open squares*, and the sum of the responses to the two individual inputs are shown as *open circles*. **e** The comparison between sum of the individual inputs at $\Delta t = 0$ and the response to paired stimuli at each timing. **f** Input timing dependency of latency to the peak of the response. *Error bars* indicate standard errors of the mean and *asterisks* indicate the level of significance: * $P < 0.05$ and ** $P < 0.01$. (For **f** the comparison is to the latency at $\Delta t = 0$.)

Our results also showed a dependence on the type of paired stimuli at $\Delta d = 5$ μm: that is, supralinear amplification is affected by which of the strong and weak inputs is proximal, even though total input strength of information is similar.

In addition, we showed that there is an area dependency on the dendrite (Experiment 2, Fig. 4). At $\Delta d = 5$ μm, supralinear amplification from inputs in the proximal area was significantly larger than that from inputs in the distal area. Because supralinear amplification showed a dependence on the temporal relation of paired stimuli (Fig. 6), there is a possibility that the proximal area on dendrites encodes information of temporal coincidence. In STDP protocols of LTP, the proximal area on dendrite shows a sharper timing sensitivity than the distal area (Froemke et al. 2005; Aihara et al. 2007). These results suggest that

the proximal area on a dendrite encodes sharp timing information (Hebb's rule) or "input–output" (STLR) information. The distal area on a dendrite has relatively broad time window, and encodes relatively broad timing information. This dependence on dendritic area may be related to the induction of associative LTP.

Now, we discuss the relation of our work to heterosynaptic associative LTP (Tsukada et al. 1996, 2007; Huang et al. 2004). In these experiments, paired stimuli were applied using micro glass electrodes. A precise stimulation area could be defined but the detailed spatial characteristics of LTP induction on the dendrite could not be examined. Huang et al. (2004) showed the induction protocol of heterosynaptic LTP. However, they did not check firing of APs, so they could not show the existence of associative LTP without a BPAP. In our study, the spatial properties of EPSP summation on a dendrite were examined quantitatively and the AP induction was confirmed by patch-clamp recording. These results are useful basic data for the spatial properties of heterosynaptic associative LTP induction without BPAPs.

Timing dependence of EPSP summation

There are few previous studies related to timing dependence (Δt) in heterosynaptic associative LTP without AP induction. Tsukada et al. (2007) reported population-level neural responses related to associative LTP from the hippocampal CA1 area by using voltage sensitive dye, and showed a temporal dependence of associative LTP induction on paired input timing for $\Delta t = -50$ to $+50$ ms. However, AP firing could not checked for technical reasons, so the temporal dependence of heterosynaptic associative LTP without AP induction was not clearly shown. Our results in this paper suggest the existence of a precise time window related to supralinear amplification and that the time window is dependent on the association timing of strong–weak paired stimuli (Δt). The time window is from $\Delta t = -20$ to $+20$ ms, and is similar to the time window in heterosynaptic associative LTP induction (Tsukada et al. 2007). From these similarities, the supralinear amplification of EPSP summation shown in this study is thought to be closely related to the mechanism for the time window for heterosynaptic associative LTP induction.

Furthermore, our results showed that the effect of supralinear amplification was largest when weak input timing overlapped with one of the three pulses in the strong input (for $\Delta t = 0$ to $+20$ ms). Neither the amplitude nor the latency of the EPSP peak showed any significant differences for $\Delta t = 0$ to $+20$ ms. These results suggest that the effect of supralinear amplification is similar when the onset of the weak input corresponds to the 1st, 2nd, or 3rd pulse in the strong input.

When the weak input was applied after the third pulse in the strong input ($\Delta t = +30$ and $+40$ ms), supralinear amplification was not observed. In contrast, when the strong input was applied after the weak input ($\Delta t = -20$ and -10 ms), supralinear amplification was observed. These results suggest that supralinear amplification of EPSP summation was dependent on the temporal order of the strong and weak inputs. These results lead to the hypothesis that the neural response of hippocampal CA1 is dependent not only on the total strength of the input, but also on temporal order information.

Temporal differences on the scale of 10 ms are critical for both supralinear summation in this experiment and the STDP protocol. In STDP protocols, LTP is induced when the neuron receives an EPSP and APs were subsequently induced. In this study, supralinear amplification was larger when the neuron received a weak input followed by a strong input. In terms of the time scale and the importance of sequential information processing, the characteristics of supralinear amplification in this study and STDP were similarly asymmetric. In addition, a delay of latency to peak amplitude was observed when the neuron received a strong input followed by a weak input ($\Delta t = +30$ and $+40$ ms). In contrast, the delay was not observed when the neuron received a weak input followed by a strong input ($\Delta t = -20$ and -10 ms). From both the nonlinear characteristics of the timing dependence of the supralinear amplification and the delay of latency, these data suggest that temporally coincident inputs induce specific channel opening and that, consequently, a boosting of EPSP summation is observed.

Molecular mechanism of supralinear amplification

In order to clarify the molecular mechanism of supralinear amplification, pharmacological experiments were carried out in this study (Fig. 5). The normalized amplification ratio at $\Delta d = 5$ and 10 μm was $<80\%$ with TTX, and $<90\%$ with Ni^{2+}. These results suggest that the voltage-gated Na^+ and Ca^{2+} channels are related to the supralinear amplification of EPSP summation.

Na^+ and Ca^{2+} channels have channel opening kinetics with a short time constant and could induce a local dendritic spike (Hille 2001). These channels were supposed to be related to the sharp uptake of the EPSP in supralinear amplification. Gasparini and Magee (2006) showed that supralinear amplification produced by spatiotemporal synchronous input was TTX sensitive. It is possible that the supralinear amplification in our results and in Gasparini and Magee (2006) have a partly common molecular mechanism. In our results, addition of AP-5 did not produce any significant effect on the normalized amplification ratio. NMDA receptors sometimes induce dendritic local

spikes in hippocampal CA1 pyramidal neurons (Gasparini et al. 2004; Remy et al. 2009). But it seems that the NMDA receptor is not related to the peak amplitude in supralinear amplification.

The decay time constant (τ) in supralinear amplification uptake was $\tau = 69.7 \pm 2.9$ ms. No significant differences in the decay time constant at $\Delta d = 5$ μm were observed with TTX or Ni^{2+}, but a significant decrease was observed ($\tau = 46.6 \pm 5.8$ ms) with AP-5. The decay time constant of the NMDA-type glutamate receptor is 50-300 ms (Hestrin et al. 1990; Lester et al. 1990), and supralinear amplification was large at $\Delta d = 5$ μm. These results suggest that NMDA channels extend the response of EPSP uptake in supralinear amplification.

Relationship to learning rule

In a Hebb type learning rule, learning is established by the coincident timing of input and output (Hebb 1949). Physiologically, the input and output of neurons correspond to EPSP and BPAP, respectively (Magee and Johnston 1997; Markram et al. 1997). STDP is learning based on Hebb type learning rules (Bi and Poo 1998, 2001), and extensive research into the interaction mechanism between BPAP and EPSP has been carried out. In a Hebb type learning rule, BPAP is modulated by voltage-gated Na^+ and K^+ channels (Hoffman et al. 1997; Stuart and Häusser 2001; Watanabe et al. 2002), and is boosted by local EPSP on dendrites (Gasparini et al. 2007). The other type of learning rule is a non-Hebb type learning rule, which is based on association among several pre- and hetero-synaptic inputs and not dependent on BPAPs, is known to be one of the LTP induction rules (Tsukada et al. 1996; Golding et al. 2002; Tsukada and Pan 2005; Tsukada et al. 2007). However, the basic mechanism for non-Hebb type LTP induction was not clear. Our results in this study show the spatiotemporal properties of supralinear amplification in EPSP summation on dendrites. The specific characteristics of supralinear amplification are as follows. (1) Supralinear amplification is induced by two spatially close inputs (within 10 μm) and (2) supralinear amplification exhibits a temporally sharp time window (<30 ms). The rapid depolarization of the membrane potential by the opening of voltage-gated cation channels induced by the opening of NMDA channels, increments the Ca^{2+} influx to the postsynapse, enhances the phosphorylation process, and induces synaptic LTP. For these reasons, our results are useful basic data about the induction mechanism of heterosynaptic associative LTP by synaptic input without BPAPs. In the hippocampal network, networks based on both Hebb and non-Hebb learning rules cooperate closely, and they process the spatiotemporal information related to learning and memory.

Acknowledgments This work was supported by the 21st Century and the Global COE Program at Tamagawa University and Grant-in-Aid for Scientific Research 17021036, 19200014, 21120006 from Ministry of Education, Culture, Sports, Science and Technology of Japan.

References

Aihara T, Abiru Y, Yamazaki Y, Watanabe H, Fukushima Y, Tsukada M (2007) The relation between spike-timing dependent plasticity and Ca^{2+} dynamics in the hippocampal CA1. Neuroscience 145:80–87

Bi G, Poo M (1998) Synaptic modifications in cultured hippocampal neurons; dependence on spike timing, synaptic strength, and postsynaptic type. J Neurosci 18:10464–10472

Bi G, Poo M (2001) Synaptic modification by correlated activity: Hebb's postulate revisited. Annu Rev Neurosci 24:139–166

Cash S, Yuste R (1999) Linear summation of excitatory inputs by CA1 pyramidal neurons. Neuron 22(2):383–394

Dan Y, Poo MM (2006) Spike timing-dependent plasticity: from synapse to perception. Physiol Rev 86:1033–1048

Froemke RC, Poo MM, Dan Y (2005) Spike-timing-dependent synaptic plasticity depends on dendritic location. Nature 434(7030):221–225

Gasparini S, Magee JC (2006) State-dependent dendritic computation in hippocampal CA1 pyramidal neurons. J Neurosci 26(7):2088–2100

Gasparini S, Migliore M, Magee JC (2004) On the initiation and propagation of dendritic spikes in CA1 pyramidal neurons. J Neurosci 24(49):11046–11056

Gasparini S, Losonczy A, Chen X, Johnston D, Magee JC (2007) Associative pairing enhances action potential back-propagation in radial oblique branches of CA1 pyramidal neurons. J Physiol 580:787–800

Golding NL, Staff NP, Spruston N (2002) Dendritic spikes as a mechanism for cooperative long-term potentiation. Nature 418(6895):326–331

Hebb DO (1949) The organization of behavior. John Wiley, New York

Hestrin S, Sah P, Nicoll RA (1990) Mechanisms generating the time course of dual component excitatory synaptic currents recorded in hippocampal slices. Neuron 5(3):247–253

Hille B (2001) Ion channels of excitable membrane, 3rd edn. Sinauer, Sunderland

Hoffman DA, Magee JC, Colbert CM, Johnston D (1997) K^+ channel regulation of signal propagation in dendrites of hippocampal pyramidal neurons. Nature 387(6636):869–875

Huang YY, Pittenger C, Kandel ER (2004) A form of long-lasting, learning-related synaptic plasticity in the hippocampus induced by heterosynaptic low-frequency pairing. Proc Natl Acad Sci USA 101(3):859–864

Kojima H, Simburger E, Nakai J, Boucsein C, Maruo T, Tsukada M, Okabe S, Aertsen Ad (2006) Development of a system for patterned rapid photolysis and 2-photon confocal microscopy. Circuit Device Mag IEEE 22(6):66–74

Lester RA, Clements JD, Westbrook GL, Jahr CE (1990) Channel kinetics determine the time course of NMDA receptor-mediated synaptic currents. Nature 346(6284):565–567

Magee JC, Cook EP (2000) Somatic EPSP amplitude is independent of synapse location in hippocampal pyramidal neurons. Nat Neurosci 3:895–903

Magee JC, Johnston D (1997) A synaptically controlled, associative signal for Hebbian plasticity in hippocampal neurons. Science 275(5297):209–213

Markram H, Lübke J, Frotscher M, Sakmann B (1997) Regulation of synaptic efficacy by coincidence of postsynaptic APs and EPSPs. Science 275(5297):213–215

Nishiyama M, Hong K, Mikoshiba K, Poo MM, Kato K (2000) Calcium stores regulate the polarity and input specificity of synaptic modification. Nature 408(6812):584–588

Remy S, Csicsvari J, Beck H (2009) Activity-dependent control of neuronal output by local and global dendritic spike attenuation. Neuron 61(6):906–916

Stuart GJ, Häusser M (2001) Dendritic coincidence detection of EPSPs and action potentials. Nat Neurosci 4(1):63–71

Tsukada M, Pan X (2005) The spatiotemporal learning rule and its efficiency in separating spatiotemporal patterns. Biol Cybern 92(2):139–146

Tsukada M, Aihara T, Saito H, Kato H (1996) Hippocampal LTP depends on spatial and temporal correlation of inputs. Neural Netw 9:1357–1365

Tsukada M, Aihara T, Kobayashi Y, Shimazaki H (2005) Spatial analysis of spike-timing-dependent LTP and LTD in the CA1 area of hippocampal slices using optical imaging. Hippocampus 15:104–109

Tsukada M, Yamazaki Y, Kojima H (2007) Interaction between the spatio-temporal learning rule (STLR) and Hebb type (HEBB) in single pyramidal cells in the hippocampal CA1 area. Cogn Neurodyn 1:1157–1167

Watanabe S, Hoffman DA, Migliore M, Johnston D (2002) Dendritic K^+ channels contribute to spike-timing dependent long-term potentiation in hippocampal pyramidal neurons. Proc Natl Acad Sci USA 99(12):8366–8371